Optically-Triggered Nanoscale Memory Effect in a Hybrid Plasmonic-Phase Changing Nanostructure

Dang Yuan Lei,*[†] Kannatassen Appavoo,[‡,§] Filip Ligmajer,[†,∥] Yannick Sonnefraud,[⊥] Richard F. Haglund, Jr.,[‡,○] and Stefan A. Maier[#]

[†]Department of Applied Physics, The Hong Kong Polytechnic University, Hong Kong, China
[‡]Interdisciplinary Materials Science Program, Vanderbilt University, Nashville, Tennessee 37235-0106, United States
[§]Centre for Functional Nanomaterials, Brookhaven National Laboratory, Upton, New York 11973, United States
[∥]Central European Institute of Technology, Brno University of Technology, Technická 10, 61669 Brno, Czech Republic
[⊥]Institut Néel, CNRS UPR2940, 25 rue des Martyrs BP166, 38042 Grenoble Cedex 9, France
[○]Department of Physics and Astronomy, Vanderbilt University, Nashville, Tennessee 37235-1807, United States
[#]Department of Physics, Imperial College London, London SW7 2AZ, United Kingdom

ABSTRACT: Nanoscale devices, such as all-optical modulators and electro-optical transducers, can be implemented in heterostructures that integrate plasmonic nanostructures with functional active materials. Here we demonstrate all-optical control of a nanoscale memory effect in such a heterostructure by coupling the localized surface plasmon resonance (LSPR) of gold nanodisk arrays to a phase-changing material (PCM), vanadium dioxide (VO_2). By latching the VO_2 in a distinct correlated metallic state during the insulator-to-metal transition (IMT), while concurrently exciting the hybrid nanostructure with one or more ultraviolet optical pulses, the entire phase

space of this correlated state can be accessed optically to modulate the plasmon response. We find that the LSPR modulation depends strongly but linearly on the initial latched state, suggesting that the memory effect encoded in the plasmon resonance wavelength is linked to the strongly correlated electron states of the VO_2. The continuous, linear variation of the electronic and optical properties of these model heterostructures opens the way to multiple design strategies for hybrid devices with novel optoelectronic functionalities, which can be controlled by an applied electric or optical field, strain, injected charge, or temperature.

KEYWORDS: surface plasmons, metal nanoparticles, vanadium dioxides, plasmonic memory effect, phase transformation
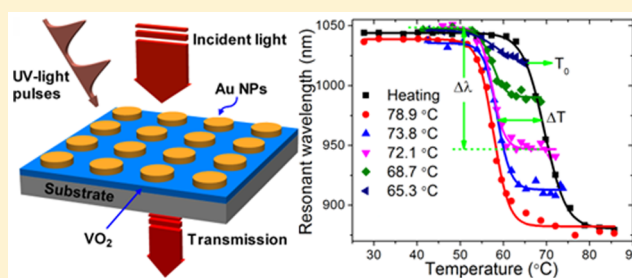
Metallic nanostructures support localized surface plasmons (LSPs) and surface-plasmon polaritons (SPPs), coherent oscillations of conduction electrons at metal−dielectric interfaces.[1] Surface plasmon excitations occur in ultrasmall mode volumes, generating high local electric fields in passive nanophotonic devices ranging from plasmon waveguides to plasmon lenses.[2,3] The optical response of plasmonic structures can be controlled by electro-optical,[4−6] thermal-optical,[7−9] or magneto-optical properties[10−13] of functional materials in close proximity. All-optical modulation of SPP propagation in metal films[14,15] and of LSPs in metal nanostructures[16−19] is also well-known. In all these schemes, however, the modulated plasmon response is necessarily transient; the metal nanostructures revert to their initial plasmonic states as soon as the external stimulus is removed. On the other hand, in many applications it would be desirable to retain functionality in a plasmonic device even after the triggering signal disappeared, allowing tunable, persistent modulation of plasmonic properties. Accessing multiple plasmonic states linearly and repeatedly by active control of plasmon modes could enhance functionality in

optoelectronic devices[20] and enable on-chip integration of optical and electronic functionalities.

Phase-change materials (PCMs), already widely used in rewritable optical data storage and nonvolatile electronic memory,[21] offer unique possibilities for persistent, reversible tuning of surface plasmons by combining PCMs with metal nanostructures to create new or multiple plasmonic functionalities. A promising PCM for this purpose is vanadium dioxide (VO_2) with its strong correlations among orbital, spin, and lattice degrees of freedom. A modest external stimulus can switch VO_2 through noncongruent electronic (from insulating to metallic) and structural (from M1 monoclinic to R rutile) phase transformations. When VO_2 is heated, this insulator-to-metal transition (IMT) occurs near a critical temperature (T_c) of 68 °C in bulk crystals[22] and thin films.[23] The IMT can also be induced mechanically,[24] electrically,[25] optically,[26] and by
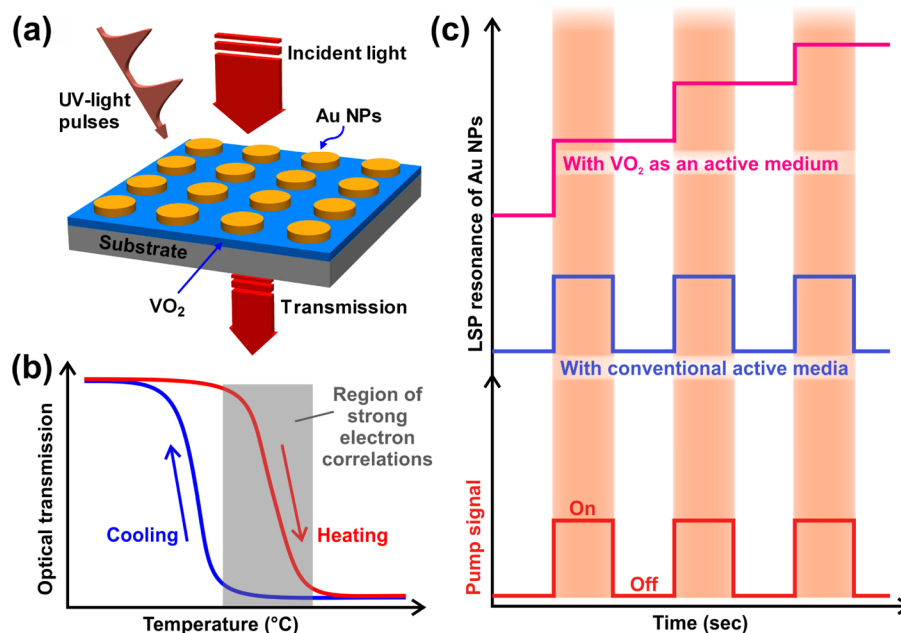
Figure 1. Model for persistent tuning of a "memplasmon" resonance. (a) Experimental schematic for the heating cycle of the phase transition: (a) Array of periodic Au nanodisks fabricated lithographically on a thin VO_2 film deposited on a SiO_2 substrate. Optical extinction measurements are conducted while successive UV-light pulses pump the VO_2 film into new states. The device is mounted on a temperature-controlled stage. (b) Hysteretic response in the optical transmission of VO_2, showing the region of strong electron−electron correlations during the heating cycle of the phase transition (shaded gray area). (c) Schematic comparison of plasmon resonance modulation schemes with conventional active media (blue) and the phase-transforming VO_2 (pink) when pumped by successive optical pump pulses (red). The strongly correlated electron state in the VO_2 is initialized and maintained by setting substrate temperature.

charge injection,[27] enabling active modulation of LSPs and SPPs in metallic nanostructures integrated with VO_2.[28−31]

Although it is generally understood how plasmons are modulated in hybrid nanostructures switched between the fully insulating and fully metallic states,[32] the potential for exploiting the entire strongly correlated phase space of a PCM has never been demonstrated at the nanoscale. In this paper, we show how the plasmonic state of a model hybrid nanostructure can be controlled by sampling different initial states within the region of strong electron correlations. We demonstrate persistent optical modulation of localized surface plasmon resonance (LSPR) in a model heterostructure comprising Au nanodisks lithographically patterned on a thin VO_2 film. Throughout the temperature window of the IMT, the VO_2 can be latched thermally in the selected strongly correlated metallic state.[33] Because of the hysteretic response of the first-order VO_2 phase transition, the LSPR can be persistently tuned by successive ultraviolet (UV) light pulses as long as the system remains in the latched, initial state. This dynamic is highly repeatable, lasts for several hours, and persists as long as the external stimulus is not varied.[34,35] Hence, the entire phase-space of this PCM can be optically addressed when the hybrid nanomaterial is latched at different starting temperatures during the IMT.

More interestingly, the subsequent temporal evolution of the LSPR depends strongly on the initial temperature from which the system is cooled, implying that the LSPR "memorizes" the initial state prepared in the hybridized plasmonic nanostructure and the strongly correlated electron state in the VO_2. It is crucial to note that here the temperature is simply a proxy for the parameter that describes the initial, latched state of the VO_2 PCM. Known properties of VO_2 suggest, therefore, that the novel resonant memory effect described here should be

observable, regardless of whether the initial state is prepared by optically, electrically, or mechanically initializing the hybrid plasmonic-phase-changing heterostructure.

MECHANISM OF PERSISTENT TUNING OF A "MEMPLASMON" RESONANCE

Figure 1 shows the hybrid plasmonic-phase-change optical material, comprising periodic arrays of Au nanostructures on a thin VO_2 film (see Figure 1a), along with a schematic of the mechanism for persistently tuning the LSPR in Au nanostructures interacting with the strongly correlated metallic state of the VO_2. When the VO_2 layer is initialized in the strong-correlation regime (shaded area, Figure 1b) by setting temperature, each successive UV-light pulse transforms more crystalline nanodomains of the VO_2 into the metallic state without recovering the initial state, manifested by a continuous change in optical transmission. This yields persistent tuning of the resonant plasmon response of Au nanostructures on top of the VO_2 film, unlike nonphase-changing, active plasmonic systems with transient resonance modulation (Figure 1c).

SAMPLE FABRICATION AND LARGE MODULATION OF LSPR VIA PHASE TRANSFORMATION

Thin VO_2 films with nominal thickness of 50 nm were fabricated on glass substrates by pulsed laser ablation of a vanadium target in 250 mTorr oxygen. Subsequent annealing of the samples at 450 °C for 40 min in 10 mTorr oxygen rendered the film stoichiometric, crystalline, and switching. A complete description of the protocol for characterizing optical response and crystal structure can be found elsewhere.[23] Four different arrays of Au nanodisks were fabricated by electron-beam

lithography on the VO_2 film; the nominal diameter D of the Au nanostructures was varied from 80 to 210 nm while keeping the thickness constant at 25 nm. The Au nanodisks were arranged on a square lattice with a pitch of 500 nm, shorter than the wavelength of interest (above 600 nm) in order to avoid diffraction effects in the transmission measurements. Figure 2a shows typical SEM images of the Au nanostructures, exhibiting reproducibility over a large area.
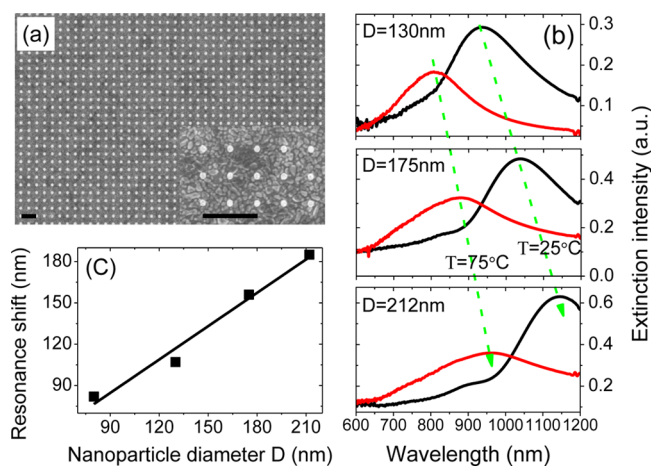

Figure 2. Modulation of localized surface plasmon resonances. (a) Plan-view SEM image of Au nanostructures patterned on a 50 nm thick VO_2 film. Inset: Nanostructure array at higher magnification. Scale bars are 1 μm in each case. (b) Measured extinction spectra of Au nanostructures for three diameters D at room- (black) and high-temperature (red). (c) Plasmon resonance peak shift due to the phase transformation of VO_2 film as a function of nanostructure diameter (black squares) with linear fit (black line).

Extinction spectra of the arrays, defined as (1 - Transmission), were acquired in an inverted optical microscope (Bruker Hyperion 2000) integrated with a Fourier-transform infrared spectrometer.[30] Extinction spectra were measured, while a Peltier thermoelectric element mounted on the sample stage cycled the VO_2 film through its phase transition by heating and cooling through a set temperature program. The external temperature was maintained within ± 0.1 °C over the entire measurement cycle in all experiments. Figure 2b shows the extinction spectra of three Au nanostructure arrays acquired below ($T = 25$ °C, black curves) and above ($T = 75$ °C, red curves) the insulator-to-metal transition of VO_2 and reveals that the LSPR of Au nanodisks experiences a substantial blue-shift due to the IMT.

The shift in LSPR for each array is plotted as a function of nanostructure diameter in Figure 2c and shows that the larger Au nanostructures also exhibit larger resonance shifts because the dielectric contrast in VO_2 during its phase transformation increases with wavelength,[36] further shifting the LSPR. In addition, the evanescent near-fields associated with the larger Au nanodisks sample a larger interaction volume in the phase-transforming VO_2 film. The ensemble of Au nanodisks is distributed over a VO_2 film having a broad range of grain sizes, each of which switches at a statistically determined temperature.[37] Hence, the average LSPR tuning should be the same for each nanostructure array and is expected to be a function of the effective or mean-field fraction of metallic phase in the underlying polycrystalline VO_2 layer.

HYSTERETIC VARIATION OF LOCALIZED SURFACE PLASMON RESONANCE

We next investigate the changes in the LSPR in Au nanostructures during the phase transformation of VO_2 by measuring extinction spectra for the array of 130 nm diameter Au nanodisks while reversibly cycling the VO_2 film across the strong-correlation regime (30−80 °C), with a resolution as small as 0.5 °C. The measured extinction spectra in Figure 3a for the hybrid system show smooth transitions in both resonance wavelength and LSPR intensity. By fitting the extinction spectra, we can map the hysteresis in resonance wavelength of the Au LSPR as a function of substrate temperature (Figure 3b). The hystereses of the Au LSPR and the far-field transmission of a bare VO_2 film (50 nm thick, Figure 3d) exhibit similar widths. The close similarity between the two hysteresis curves indicates that the evolution of the Au LSPR tracks the phase-transition properties of the underlying VO_2 film and can properly be used as an optical marker for the change in local optical properties in the phase-changing material. The slight reduction in thermal hysteresis width ΔT for the LSPR compared to that for the bare VO_2 film can be attributed to the presence of additional nucleation sites at the Au/VO_2 interface, which facilitate the phase-transformation of VO_2 by reducing the phase-transition barrier energy.[38]

To further correlate the LSPR modulation with the phase changing dynamics of VO_2, Figure 3c and e show, respectively, the plasmon resonance wavelength of the Au nanodisks and the transmission intensity of the bare VO_2 film as a function of the VO_2 metallic fraction that is determined from the hysteretic parameters shown in Figure 3b,d by using the method described in ref 48. The results demonstrate a linear relationship between both plasmon resonance wavelength and transmission intensity, and the metallic fraction of VO_2, thereby indicating a continuous, linear variation of the electronic and optical properties of both systems.

PERSISTENT OPTICAL TUNING OF LSPR USING SUCCESSIVE UV-LIGHT PULSES

Apart from the external temperature, UV-light pulses can be used to trigger the insulator-to-metal transition from the prepared initial state because VO_2 has strong absorption in the UV range, as indicated by the large imaginary component of its dielectric function.[36] Successive UV-illumination pulses also increase the areal density of the metallic phase in VO_2, gradually changing the average dielectric response of the film and consequently altering the persistent tuning characteristic of the LSPR. After a sufficiently long illumination time, the metallic nanopuddles connect percolatively and leave the VO_2 film in a pure metallic phase.

The hysteresis during the VO_2 phase transition allows for persistent tuning of the Au nanostructure LSPR when the external temperature is biased within the temperature range where strong electron−electron correlation exists. To demonstrate this effect, we prepared the VO_2 film in a strongly correlated metal state by maintaining the array and its substrate at a sequence of constant temperatures. The system was then illuminated by successive UV-light pulses either with a constant power density and varying pulse durations or with different power densities at constant pulse duration (varying fluence). After each such pulse sequence, we measured the extinction spectrum of the Au nanodisk array. Control experiments were also performed at two temperatures well below and above the
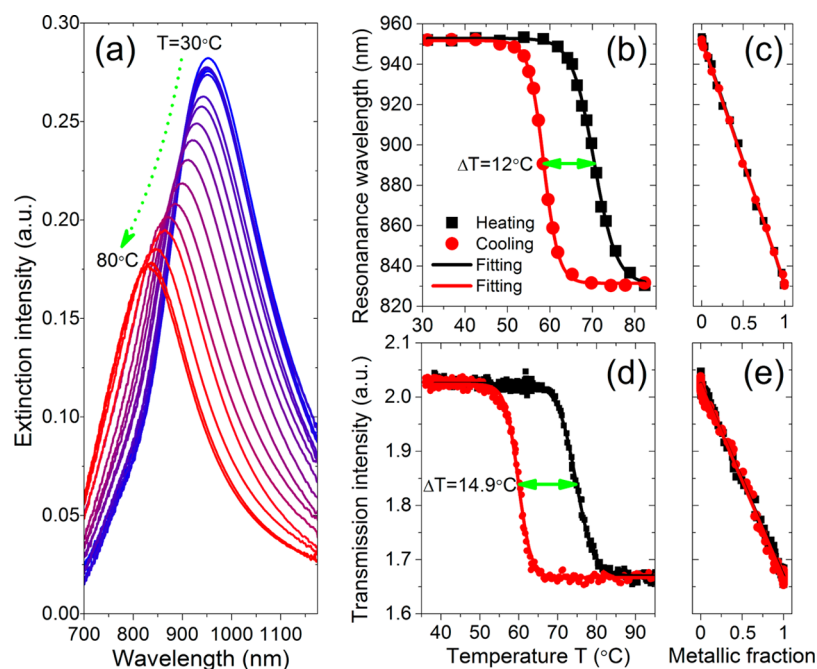
Figure 3. Hysteretic response of localized surface plasmon resonance. (a) Temperature-dependent extinction spectra for Au nanostructures of 130 nm diameter on VO_2 through the heating cycle with a temperature increment of 0.5 °C around the phase-transition temperature. (b) Plasmon resonance hysteresis curve for the same structure extracted from (a). (d) Ensemble transmission hysteresis curve of a 50 nm VO_2 film. Here the sample was illuminated by a tungsten lamp and the integrated, unpolarized transmission intensity was recorded as a function of temperature using an InGaAs photodetector. In both (b) and (d), the black squares and red circles are the measured results for heating and cooling cycles, respectively, while the black and red solid lines are sigmoidal functions fits to the measured data. The green double-headed arrows define the thermal hysteresis width for each system. (c, e) Plasmon resonance wavelength from (b) and transmission intensity from (d) as a function of the VO_2 effective metallic fraction, respectively.

critical temperature of VO_2, and the corresponding extinction spectra were recorded for comparison with those collected at temperatures within the strongly correlated range. To verify that the plasmon resonance shift observed in Au nanodisks was due to the altered dielectric response of VO_2, spectroscopic ellipsometry[39] was used to characterize a bare VO_2 film of the same thickness (50 nm) and the change in dielectric response was measured using the same UV-illumination protocol used for the hybrid plasmonic system. The dielectric function of VO_2 was extracted by fitting the ellipsometric data with a sum of one Gaussian and one Lorentz oscillator under a global-minimization algorithm.

Figure 4a shows how the plasmon resonance is modulated by UV illumination for different pulse durations at constant power density (90 mW/cm^2) while keeping the hybrid system at 64 and 68 °C, respectively. The LSPR wavelength extracted from each extinction spectrum as a function of total illumination time exhibits a substantial blue-shift after the initial few pulses, followed by a gradual saturation in the resonance wavelength for much longer pulse durations. Such behavior contrasts sharply with results from the control experiments performed at 27 °C (not shown) and 77 °C, in which the LSPR wavelength shows no sensitivity whatsoever to the UV illumination. Figure 4b shows similar results when the LSPR wavelength is modulated by UV-light pulses of constant duration (10 s) but with various power densities: A large blue-shift and subsequent resonance saturation also occurs when gradually increasing the power density of single UV-light pulses. The inset in Figure 4b plots the dispersive refractive index of the bare VO_2 film extracted from spectroscopic ellipsometry as a function of the UV-illumination power density at a constant temperature of 65
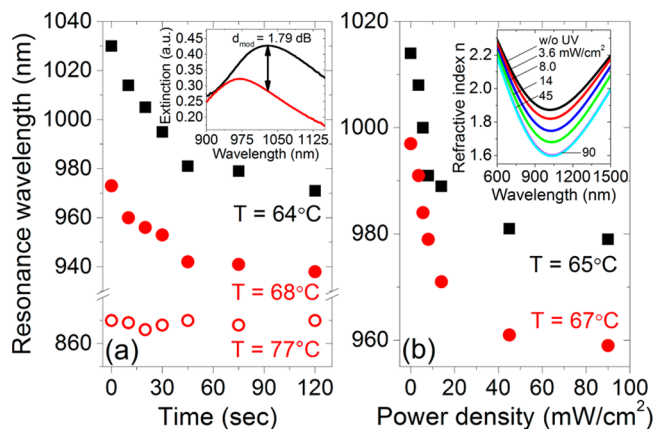

Figure 4. Persistent optical tuning of LSPR by UV-light pulses. (a) Plasmon resonance wavelength of the Au nanodisks of 175 nm diameter on the VO_2 film as a function of the total UV illumination time with a constant power density of 90 mW/cm^2, while the whole sample was thermally latched at two different temperatures within the phase transition region, 64 °C (black squares) and 68 °C (red circles), and also above (77 °C, red empty circles). Each of the first three pulses has a duration of 10 s, followed by another two pulses of 15 s, respectively, and the last one of 45 s. Inset shows the measured extinction spectra for the sample latched at 64 °C before (black) and after (red) 120 s UV illumination, and the modulation depth (i.e., extinction ratio) at a wavelength of 1029 nm is calculated to be 1.79 dB. (b) Resonance shift for the same structure as a function of the power density of each UV-light pulse of 10 s duration. Inset shows the dispersive refractive index for a 50 nm bare VO_2 film illuminated at the same conditions as above.
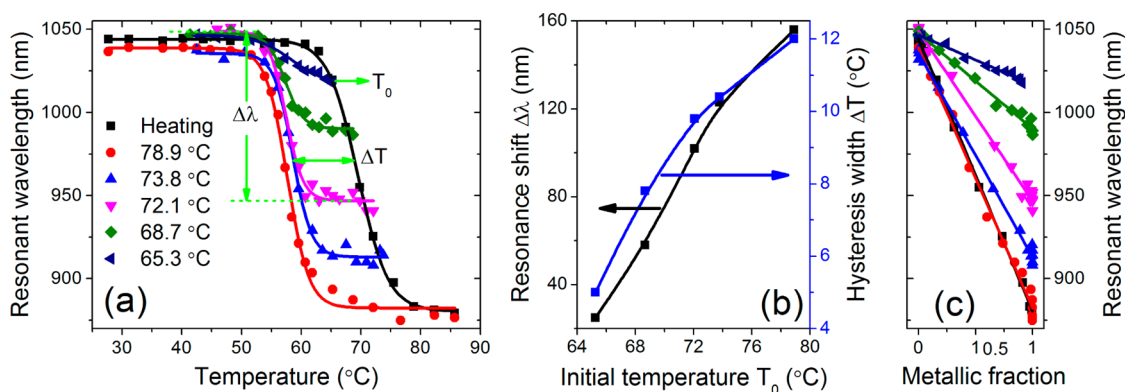
Figure 5. Temperature evolution of LSPR retracing the initial temperature states. (a) LSPR wavelength evolutions for 175 nm-diameter Au nanodisks on VO_2 through cooling cycles starting from different initial temperatures T_0 (red circles to dark-blue left-triangles). The black squares are the resonance positions through the heating cycle. The quantities ΔT and $\Delta\lambda$ represent the thermal hysteresis width and the resonance shift amplitude for each initial state of the film, with results shown in (b) as a function of initial bias temperature T_0. Solid lines in (a) are sigmoidal fits to the measured data points, while black and blue solid lines in (b) are guides to the eye. The plasmon resonance wavelength extracted from (a) for different initial temperatures and heating cycles are replotted in (c) as a function of the effective metallic fraction of the VO_2.

°C, which reveals a gradual decrease in the refractive index of VO_2 in the wavelength range of interest and accounts for the observed blue-shift in the LSPR of Au nanostructures.

In analogy to the general definition of modulation depth for silicon photonic modulators,[40] here we define the extinction ratio $10 \log(I_0/I_{UV})$ as the modulation depth for the Au/VO_2 hybrid heterostructure, where I_0 and I_{UV} are the extinction intensities at a specific plasmonic wavelength for the system thermally latched within the phase transition region of VO_2 before and after a certain period of UV illumination, respectively. The inset of Figure 4a shows the measured extinction spectra for the Au nanodisks of 175 nm diameter on the VO_2 film before and after 120 s, 90 mW/cm^2 UV illumination under the bias temperature of 64 °C, from which the modulation depth at the plasmonic wavelength 1029 nm is calculated to be 1.79 dB. Note that this value might be underestimated because in the extinction calculation the transmission of each Au nanodisk array was normalized with respect to the transmitted light through a bare VO_2 area in close proximity to the array. This implies that the extinction contribution from the VO_2 itself has not been taken into account in the calculation of modulation depth.

EVOLUTION TRACES OF LSPR REGISTERING THE INITIAL TEMPERATURE STATES

In a temperature-controlled memristive device driven by the VO_2 phase transition, the resistance takes different paths for cooling and heating cycles; in particular, the time evolution of the resistance depends strongly on the bias temperature from which the cooling cycle starts.[41] This means that the initial temperature states or the associated information stored in the system can be retrieved by monitoring the evolving path of the system resistance. More generally, in a memristive metal/oxide/metal nanodevice, this corresponds to the hysteretic response of $I-V$ curves in which the applied voltage and resultant current follow a highly nonlinear relationship and the evolutionary history of the current−voltage relationship depends on the initial bias voltage.[42,43]

The optical-frequency, plasmon memory resonance described in this experiment exhibits features analogous to such memristive behavior. Figure 5a plots LSPR wavelength as a function of temperature during the cooling cycle starting from

different bias temperatures. Each such evolutionary path is unique, yielding a characteristic parameter pair, thermal hysteresis width and resonance shift, for each bias temperature (Figure 5b). The unique evolution of the LSPR can also be observed by plotting the plasmon resonance wavelengths (extracted from Figure 5a for each different initial temperature and heating cycle) as a function of the effective metallic fraction of VO_2 (Figure 5c). The strong similarity between a memristive response[41−43] and the behavior of the hybrid plasmonic system further supports the idea that an optical-frequency plasmon resonance of the metallic nanostructure can store and read out the "memory" of the initial hybridized state in a broad range of phase-transforming materials like VO_2.

DISCUSSION

The hysteretic nature of the first-order phase transition in VO_2 is the key to realizing the persistent plasmon resonance tuning in practice. In this experimental configuration a bias temperature somewhere in the transition region from insulator to metal, that is, between 60 and 80 °C (Figure 4), initializes the VO_2 in a strongly correlated state. The UV-modulation experiments reveal that the LSPR of Au nanostructures is "pinned" at a wavelength defined by the initial state of the VO_2 film and the duration of illumination. Successive UV-light pulses drive the LSPR to a new wavelength as more VO_2 domains are switched from insulating to metallic. The hysteretic response of this hybridized heterostructure after the triggering impulse fades away (as demonstrated in Figure 5) is then essential for the long-lasting memory of the UV-light induced change which is "imprinted" into the LSPR frequency.

As noted in the discussion of Figure 5, this LSPR memory effect in metal nanostructures resembles in some ways the memory capacitance and memristive responses of VO_2 in memory metamaterials[44] and phase-transition-based memory devices.[41] However, the plasmon memory resonance observed here at optical to near-infrared frequencies is based on the hybrid response of the Au nanodisks and the hysteretic response of VO_2. This is distinctly different from the metamaterial memristive system[44] that exploits the hysteresis in VO_2 dielectric constants at terahertz or microwave frequencies. Finally, it should be noted that, although UV pulses of a few tens of seconds were used in this study, the

phase transition dynamics of VO_2 is not intrinsically restricted to slow time scales. The absorbed UV light in the present experiment causes both transient local heating and electronic excitation, leading to the formation of new metallic nanopuddles in the insulating VO_2 host and driving the film toward completed formation of the metallic, rutile phase. If the UV energy density is high enough to cause the transition to occur by local heating, the reversion from the rutile metallic state to the insulating state could require nanoseconds to microseconds. If, on the other hand, the UV light pulse is ultrashort[26] and the transition proceeds primarily through electronic excitation to the recently observed metallic monoclinic state,[45−47] the complete transition cycle could then occur on a picosecond time scale without a structural phase transition, making it possible to consider practical applications. Another potential route to an ultrafast device using the hybrid material system demonstrated here would be by electron injection initiated by resonant excitation of a noble-metal nanoparticle.[27]

The plasmon memory resonance effect can be generalized in a number of ways. Because the critical temperature and the slope of the hysteresis curve for a VO_2 film can be substantially altered by impurity doping,[48] electrical bias,[49] charge injection,[27] or substrate-induced strain,[50] even for the ultrafast laser-driven phase transition,[51] a plasmon memory device can, in principle, be operated at lower temperatures, and over a broader temperature range, than what is demonstrated here. Conversely, since the initial strongly correlated metal state can be prepared by applied bias voltage, charge injection, strain, or laser illumination, a plasmon memory device can be designed to operate at a constant temperature. The thermal hysteresis width of the IMT in VO_2 can be altered by changing fabrication parameters to yield differing grain sizes in a film,[23] ordered arrays of nanostructures,[30] or strained one-dimensional nanostructures.[24] Flexible control over both the transition temperature and hysteresis width of the VO_2 also allows for stable modulation of the plasmon resonance wavelength.

Other nanostructure configurations can easily be imagined: For example, one could imagine a double-layer lithography[32] procedure in which one would remove all the VO_2 outside the range of the plasmon near-field, leaving a double-layer Au/VO_2 heterostructure array with a defined pitch. Finally, since the phase transformation in VO_2 is associated with strong electron−electron correlations, the plasmon memory resonance offers a unique opportunity to monitor the interaction between the collective oscillation of free electrons in the surface plasmons and strongly correlated electrons during the interband transitions in VO_2.[52]

Although these experiments employed Au nanostructure arrays, the behavior observed here should also occur in individual metal nanostructures and be observable using single-particle spectroscopy to monitor the plasmon resonance shift. In fact, single-particle studies could explore the metal-to-insulator phase-transition on the nanoscale by monitoring electromagnetic near fields associated with localized surface plasmons. For example, an individual metal nanostructure used as a nanoprobe could detect coexisting insulating and metallic phases in VO_2 and the divergence of the real dielectric function near the onset of the insulator-to-metal transition.

CONCLUSION

We have demonstrated a novel plasmon memory resonance by hybridizing the surface plasmon resonance in metallic nanostructures with the strong electron−electron correlation effects in a phase-changing VO_2 thin film. Analogous to the memristive response of VO_2, this plasmon memory resonance exhibits persistent tuning of the resonance frequency when illuminated by ultraviolet light, in contrast to plasmon modulation schemes using conventional active media. The temperature and temporal evolution of the observed mem-plasmon resonance depends critically on the correlated initial state of the VO_2 and, thus, enables reversible operation of the device to reinitialize the hybrid plasmonic memory material.

This memory effect on the resonance frequency of a plasmonic nanostructure due to the strong electron−electron correlations in VO_2 exhibits an optical analog of memory circuit devices, the plasmon memory resonance, but now in the optical to near-infrared range rather than the microwave and THz range.[41−43] Nanoscale integration of plasmonic structures with phase-changing materials, such as VO_2, could enable further miniaturization of an entire class of memory devices for next-generation nanophotonic circuitry, simply because such devices would work at shorter wavelengths than THz or microwave-based devices. The dual-excitation scheme presented in this work could potentially be extended to other hybrid plasmonic/PCM systems, incorporating the controlled metal-to-insulator phase transition in $NdNiO_3$,[53] colossal magnetoresistance in perovskite materials like $LaMnO_3$[54] and $Pr_{0.7}Ca_{0.3}MnO_3$.[55]

Combined with novel nanostructure architectures[32] and excitation schemes,[56] this proof-of-concept demonstration has a significant impact on the possibilities for transferring the basic concepts in conventional circuits, such as memristive behavior and memory capacitance, to nanoscale optical devices operating in the visible and near-infrared regimes.

AUTHOR INFORMATION

Corresponding Author
*E-mail: dylei@polyu.edu.hk.
Notes
The authors declare no competing financial interest.

REFERENCES

(1) Maier, S. A. *Plasmonics: Fundamentals and Applications*; Springer: New York, 2007.
(2) Bozhevolnyi, S. I.; Volkov, V. S.; Devaux, S.; Laluet, J.-Y.; Ebbesen, T. W. Channel plasmon subwavelength waveguide components including interferometers and ring resonators. *Nature* **2006**, *440*, 508.
(3) Liu, Z.; Steele, J. M.; Srituravanich, W.; Pikus, Y.; Sun, C.; Zhang, X. Focusing surface plasmons with a plasmonic lens. *Nano Lett.* **2005**, *5*, 1726−1729.
(4) Müller, J.; Sönnichsen, C.; von Poschinger, H.; von Plessen, G.; Klar, T. A.; Feldmann, J. Electrically controlled light scattering with single metal nanoparticles. *Appl. Phys. Lett.* **2002**, *81*, 171.

(5) Dicken, M. J.; Sweatlock, L. A.; Pacifici, D.; Lezec, H. J.; Bhattacharya, K.; Atwater, H. A. Electrooptic modulation in thin film barium titanate plasmonic interferometers. *Nano Lett.* **2008**, *8*, 4048−4052.

(6) Neutens, P.; Van Dorpe, P.; De Vlaminck, I.; Lagae, L.; Borghs, G. Electrical detection of confined gap plasmons in metal−insulator−metal waveguides. *Nat. Photonics* **2009**, *3*, 283.

(7) Suh, J. Y.; Donev, E. U.; Lopez, R.; Feldman, L. C.; Haglund, R. F. Modulated optical transmission of subwavelength hole arrays in metal-VO$_2$ films. *Appl. Phys. Lett.* **2006**, *88*, 133115.

(8) Lei, D. Y.; Appavoo, K.; Sonnefraud, Y.; Haglund, R. F., Jr.; Maier, S. A. Single-particle plasmon resonance spectroscopy of phase transition in vanadium dioxide. *Opt. Lett.* **2010**, *35*, 3988.

(9) Ren, F.; Wang, X.; Wang, A. X. Thermo-optic modulation of plasmonic bandgap on metallic photonic crystal slab. *Appl. Phys. Lett.* **2013**, *102*, 181101.

(10) Temnov, V. V.; Armelles, G.; Woggon, U.; Guzatov, D.; Cebollada, A.; Garcia-Martin, A.; Garcia-Martin, J.-M.; Thomay, T.; Leitenstorfer, A.; Bratschitsch, R. Active magneto-plasmonics in hybrid metal−ferromagnet structures. *Nat. Photonics* **2010**, *4*, 107.

(11) Belotelov, V. I.; Akimov, I. A.; Pohl, M.; Kotov, V. A.; Kasture, S.; Vengurlekar, A. S.; Gopal, A. V.; Yakovlev, D. R.; Zvezdin, A. K.; Bayer, M. Enhanced magneto-optical effects in magnetoplasmonic crystals. *Nat. Nanotechnol.* **2011**, *6*, 370.

(12) Bonanni, V.; Bonetti, S.; Pakizeh, T.; Pirzadeh, Z.; Chen, J.; Nogués, J.; Vavassori, P.; Hillenbrand, R.; Åkerman, J.; Dmitriev, A. Designer magnetoplasmonics with nickel nanoferromagnets. *Nano Lett.* **2011**, *11*, 5333−5338.

(13) Chin, J. Y.; Steinle, T.; Wehlus, T.; Dregely, D.; Weiss, T.; Belotelov, V. I.; Stritzker, B.; Giessen, H. Nonreciprocal plasmonics enables giant enhancement of thin-film Faraday rotation. *Nat. Commun.* **2013**, *4*, 1599.

(14) MacDonald, K. F.; Sámson, Z. L.; Stockman, M. I.; Zheludev, N. I. Ultrafast active plasmonics. *Nat. Photonics* **2009**, *3*, 55.

(15) Pacifici, D.; Lezec, H. J.; Atwater, H. A. All-optical modulation by plasmonic excitation of CdSe quantum dots. *Nat. Photonics* **2007**, *1*, 402.

(16) Utikal, T.; Stockman, M. I.; Heberle, A. P.; Lippitz, M.; Giessen, H. All-optical control of the ultrafast dynamics of a hybrid plasmonic system. *Phys. Rev. Lett.* **2010**, *104*, 113903.

(17) Wurtz, G. A.; Pollard, R.; Hendren, W.; Wiederrecht, G. P.; Podolskiy, V. A.; Zayats, A. V. Designed ultrafast optical nonlinearity in a plasmonic nanorod metamaterial enhanced by nonlocality. *Nat. Nanotechnol.* **2011**, *6*, 107.

(18) Abb, M.; Albella, P.; Aizpurua, J.; Muskens, O. L. All-optical control of a single plasmonic nanoantenna-ITO hybrid. *Nano Lett.* **2011**, *11*, 2457−2463.

(19) Zhu, Y.; Hu, X.; Fu, Y.; Yang, H.; Gong, Q. Ultralow-power and ultrafast all-optical tunable plasmon-induced transparency in metamaterials at optical communication range. *Sci. Rep.* **2013**, *3*, 2338.

(20) Hoessbacher, C.; Fedoryshyn, Y.; Emboras, A.; Melikyan, A.; Kohl, M.; Hillerkuss, D.; Hafner, C.; Leuthold, J. The plasmonic memristor: a latching optical switch. *Optica* **2014**, *1*, 198−202.

(21) Wuttig, M.; Yamada, N. Phase-change materials for rewriteable data storage. *Nat. Mater.* **2007**, *6*, 824.

(22) Morin, F. J. Oxides which show a metal-to-insulator transition at the Neel temperature. *Phys. Rev. Lett.* **1959**, *3*, 34−36.

(23) Suh, J. Y.; Lopez, R.; Feldman, L. C.; Haglund, R. F. Semiconductor to metal phase transition in the nucleation and growth of VO$_2$ nanoparticles and thin films. *J. Appl. Phys.* **2004**, *96*, 1209.

(24) Wei, J.; Wang, Z.; Chen, W.; Cobden, D. H. New aspects of the metal−insulator transition in single-domain vanadium dioxide nanobeams. *Nat. Nanotechnol.* **2009**, *4*, 420.

(25) Qazilbash, M. M.; Li, Z. Q.; Podzorov, V.; Brehm, M.; Keilmann, F.; Chae, B. G.; Kim, H. T.; Basov, D. N. Electrostatic modification of infrared response in gated structures based on VO$_2$. *Appl. Phys. Lett.* **2008**, *92*, 241906.

(26) Cavalleri, A.; Dekorsy, Th.; Chong, H. H. W.; Kieffer, J. C.; Schoenlein, R. W. Evidence for a structurally-driven insulator-to-metal

(27) Appavoo, K.; Wang, B.; Brady, N. F.; Seo, M.; Nag, J.; Prasankumar, R. P.; Hilton, D. J.; Pantelides, S. T.; Haglund, R. F., Jr. Ultrafast phase transition via catastrophic phonon collapse driven by plasmonic hot-electron injection. *Nano Lett.* **2014**, *14*, 1127−1133.

(28) Dicken, M. J.; Aydin, K.; Pryce, I. M.; Sweatlock, L. A.; Boyd, E. M.; Walavalkar, S.; Ma, J.; Atwater, H. A. Frequency tunable near-infrared metamaterials based on VO$_2$ phase transition. *Opt. Express* **2009**, *17*, 18330.

(29) Seo, M.; Kyoung, J.; Park, H.; Koo, S.; Kim, H.-S.; Bernien, H.; Kim, B. J.; Choe, J. H.; Ahn, Y. H.; Kim, H.-T.; Park, N.; Park, Q.-H.; Ahn, K.; Kim, D.-S. Active terahertz nanoantennas based on VO$_2$ phase transition. *Nano Lett.* **2010**, *10*, 2064−2068.

(30) Appavoo, K.; Lei, D. Y.; Sonnefraud, Y.; Wang, B.; Pantelides, S. T.; Maier, S. A.; Haglund, R. F., Jr. Role of defects in the phase transition of VO$_2$ nanoparticles probed by plasmon resonance spectroscopy. *Nano Lett.* **2012**, *12*, 780−786.

(31) Ye, J.; Van Dorpe, P. Plasmonic behaviors of gold dimers perturbed by a single nanoparticle in the gap. *Nanoscale* **2012**, *4*, 7205.

(32) Appavoo, K.; Haglund, R. F., Jr. Polarization selective phase-change nanomodulator. *Sci. Rep.* **2014**, *4*, 6771.

(33) Qazilbash, M. M.; Brehm, M.; Chae, B. G.; Ho, P.-C.; Andreev, G. O.; Kim, B.-J.; Yun, S. J.; Balatsky, A. V.; Maple, M. B.; Keilmann, F.; Kim, H.-T.; Basov, D. N. Mott transition in VO$_2$ revealed by infrared spectroscopy and nano-imaging. *Science* **2007**, *318*, 1750.

(34) Coy, H.; Cabrera, R.; Sepúlveda, N.; Fernández, F. E. Optoelectronic and all-optical multiple memory states in vanadium dioxide. *J. Appl. Phys.* **2010**, *108*, 113115.

(35) Gurvitch, M.; Luryi, S.; Polyakov, A.; Shabalov, A. Nonhysteretic behavior inside the hysteresis loop of VO2 and its possible application in infrared imaging. *J. Appl. Phys.* **2009**, *106*, 104504.

(36) Verleur, H. W.; Barker, A. S.; Berglund, C. N. Optical properties of VO$_2$ between 0.25 and 5 eV. *Phys. Rev.* **1968**, *172*, 788.

(37) Lopez, L.; Feldman, L. C.; Haglund, R. F. Size-dependent optical properties of VO$_2$ nanoparticle arrays. *Phys. Rev. Lett.* **2004**, *93*, 177403.

(38) Appavoo, K.; Haglund, R. F., Jr. Detecting nanoscale size dependence in VO$_2$ phase transition using a split-ring resonator metamaterial. *Nano Lett.* **2011**, *11*, 1025−1031.

(39) Lei, D. Y.; Kéna-Cohen, S.; Zou, B.; Petrov, P. K.; Sonnefraud, Y.; Breeze, J.; Maier, S. A.; Alford, N. M. Spectroscopic ellipsometry as an optical probe of strain evolution in ferroelectric thin films. *Opt. Express* **2012**, *20*, 4419.

(40) Reed, G. T.; Mashanovich, G.; Gardes, F. Y.; Thomson, D. J. Silicon optical modulators. *Nat. Photonics* **2010**, *4*, 518.

(41) Driscoll, T.; Kim, H.-T.; Chae, B.-G.; Di Ventra, M.; Basov, D. N. Phase-transition driven memristive system. *Appl. Phys. Lett.* **2009**, *95*, 043503.

(42) Strukov, D. B.; Snider, G. S.; Stewart, D. R.; Williams, R. S. The missing memristor found. *Nature* **2008**, *453*, 80.

(43) Yang, J. J.; Pickett, M. D.; Li, X.; Ohlberg, D. A. A.; Stewart, D. R.; Williams, R. S. Memristive switching mechanism for metal/oxide/metal nanodevices. *Nat. Nanotechnol.* **2008**, *3*, 429.

(44) Driscoll, T.; Kim, H.-T.; Chae, B.-G.; Kim, B.-J.; Lee, Y.-W.; Jokerst, N. M.; Palit, S.; Smith, D. R.; Di Ventra, M.; Basov, D. N. Memory metamaterials. *Science* **2009**, *325*, 1518.

(45) Laverock, J.; Kittiwatanakul, S.; Zakharov, A. A.; Niu, Y. R.; Chen, B.; Wolf, S. A.; Lu, J. W.; Smith, K. E. Direct observation of decoupled structural and electronic transitions and an ambient pressure monocliniclike metallic phase of VO$_2$. *Phys. Rev. Lett.* **2014**, *113*, 216402.

(46) Morrison, V. R.; Chatelain, R. P.; Tiwari, K. L.; Hendaoui, A.; Bruhacs, A.; Chaker, M.; Siwick, B. J. A photoinduced metal-like phase of monoclinic VO$_2$ revealed by ultrafast electron diffraction. *Science* **2014**, *346*, 445−448.

(47) Wegkamp, D.; Herzog, M.; Xian, L.; Gatti, M.; Cudazzo, P.; McGahan, C. L.; Marvel, R. E.; Haglund, R. F.; Rubio, A.; Wolf, M.;

Stähler, J. Instantaneous band-gap collapse in photoexcited monoclinic VO_2 due to photocarrier doping. *Phys. Rev. Lett.* **2014**, *113*, 216401.

(48) Shibuya, K.; Kawasaki, M.; Tokura, Y. Metal-insulator transition in epitaxial $V_{1-x}WxO_2$ ($0 \leq x \leq 0.33$) thin films. *Appl. Phys. Lett.* **2010**, *96*, 022102.

(49) Yang, Z.; Hart, S.; Ko, C.; Yacoby, A.; Ramanathan, S. Studies on electric triggering of the metal-insulator transition in VO_2 thin films between 77 and 300 K. *J. Appl. Phys.* **2011**, *110*, 033725.

(50) Wu, J.; Gu, Q.; Guiton, B. S.; de Leon, N. P.; Ouyang, L.; Park, H. Strain-induced self organization of metal−insulator domains in single-crystalline VO_2 nanobeams. *Nano Lett.* **2006**, *6*, 2313−2317.

(51) Pashkin, A.; Kübler, C.; Ehrke, H.; Lopez, R.; Halabica, A.; Haglund, R. F., Jr.; Huber, R.; Leitenstorfer, A. Ultrafast insulator-metal phase transition in VO_2 studied by multiterahertz spectroscopy. *Phys. Rev. B: Condens. Matter Mater. Phys.* **2011**, *83*, 195120.

(52) Ferrara, D. W.; Nag, J.; MacQuarrie, E. R.; Kaye, A. B.; Haglund, R. F., Jr. Plasmonic probe of the semiconductor to metal phase transition in vanadium dioxide. *Nano Lett.* **2013**, *13*, 4169−4175.

(53) Asanuma, S.; Xiang, P.-H.; Yamada, H.; Sato, H.; Inoue, I. H.; Akoh, H.; Sawa, A.; Ueno, K.; Shimotani, H.; Yuan, H.; Kawasaki, M.; Iwasa, Y. Tuning of the metal-insulator transition in electrolyte-gated $NdNiO_3$ thin films. *Appl. Phys. Lett.* **2010**, *97*, 142110.

(54) Ramirez, A. P. Colossal magnetoresistance. *J. Phys.: Condens. Matter* **1997**, *9*, 8171−8199.

(55) Fiebig, M.; Miyano, K.; Tomioka, Y.; Tokura, Y. Visualization of the local insulator-metal transition in $Pr_{0.7}Ca_{0.3}MnO_3$. *Science* **1998**, *280*, 1925−1928.

(56) Aouani, H.; Rahmani, M.; Navarro-Cia, M.; Maier, S. A. Third-harmonic-upconversion enhancement from a single semiconductor nanoparticle coupled to a plasmonic antenna. *Nat. Nanotechnol.* **2014**, *9*, 290−294.